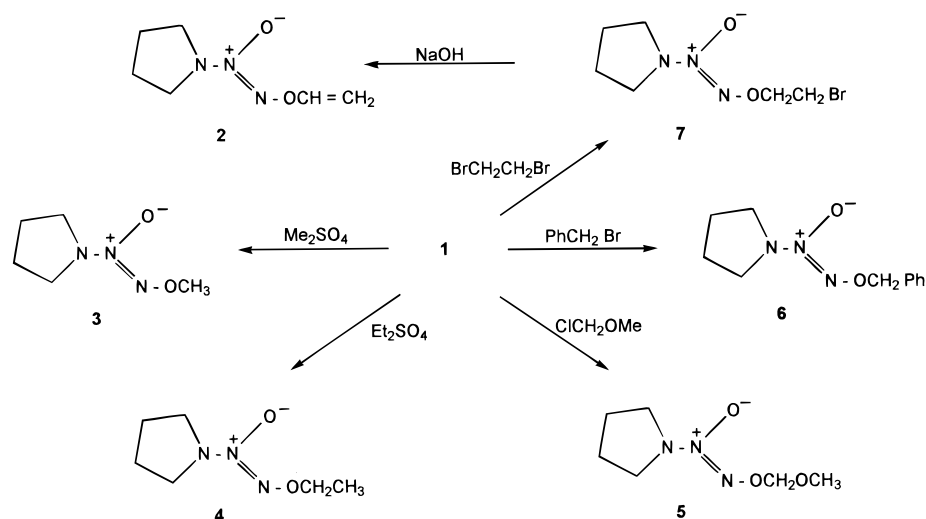
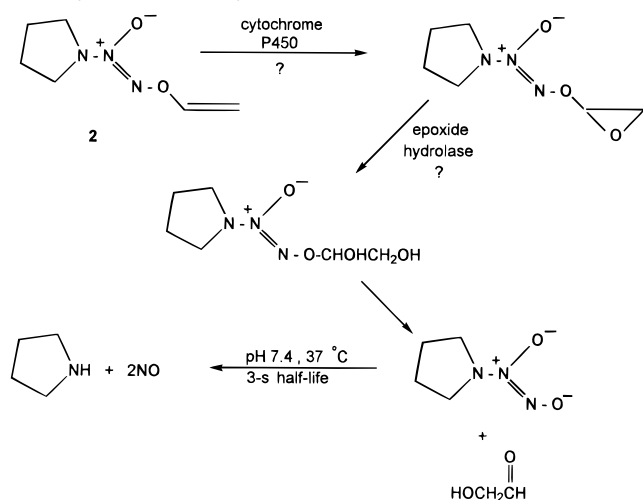


Scheme 1. Synthesis of Prodrug Candidates**Scheme 2.** Postulated Mechanism of Liver-Selective Nitric Oxide Generation on Metabolism of **2** (V-PYRRO/NO) by Hepatic Enzymes *in Vivo*^a

^a Experiments aimed at confirming the involvement of cytochrome P450 in the metabolic activation of **2** are currently in progress (collaboration with D. Gergel, V. Misik, P. Riesz, and A. Cederbaum).

We speculated that *O*-alkenyl and -alkyl derivatives of **1**, previously shown to be substituted at the terminal (*O*²) oxygen,⁶ should be useful for targeting the liver. Accordingly, we synthesized the selection of candidate prodrugs shown in Scheme 1 for tests of this hypothesis. We predicted that hepatic cytochromes P450,⁷ known to be capable of epoxidizing vinyl ethers,⁸ might initiate the metabolic activation of **2** via the mechanism shown in Scheme 2. If subsequent hydrolysis of the resulting oxirane (possibly with catalysis by epoxide hydrolase, also prevalent in the liver⁹) and fragmentation of the intermediate hemiacetal to regenerate **1** were sufficiently rapid, NO release should be largely confined to the site of metabolism. Hemiacetals produced by hydroxylation of the protecting group's α carbon during P450-catalyzed dealkylation of ethers **3–6** should be similarly reactive.⁷

As an initial test of these hypotheses, compounds **2–6** were incubated with cultured hepatocytes, and accumulation of the NO oxidation products, nitrite and nitrate, was monitored over 6 h. The compounds

showed varying degrees of enzymatic and/or nonenzymatic conversion to NO, as summarized in Figure 1, but **2** proved to be metabolized with special efficiency; the total concentration of nitrite and nitrate produced during a 6-h incubation of this compound with hepatocytes reached 12.5 ± 1.2 and $40.8 \pm 10.0 \mu\text{M}$ at initial concentrations of 0.1 and 1 mM, respectively. For this reason, we chose **2** (V-PYRRO/NO) for further study.

Hepatocyte-Selective Metabolism of V-PYRRO/NO *in Vitro*

We next confirmed that V-PYRRO/NO released NO in a hepatocyte-selective manner. When monolayer cultures of hepatocytes, liver nonparenchymal cells (endothelial cells plus Kupffer cells), arterial vascular smooth muscle cells, vascular endothelial cells, or the murine macrophage cell line RAW 264.7 were incubated with 1 mM V-PYRRO/NO for 24 h, significant increases in total $\text{NO}_2^- + \text{NO}_3^-$ levels were detected only in the hepatocyte cultures (Figure 2A). A 1:1 ratio of NO_2^- to NO_3^- (data not shown) was obtained; this is similar to the ratio of NO_2^- to NO_3^- released from hepatocytes stimulated to express the inducible NO synthase (iNOS).¹⁰ The release of NO_2^- from hepatocytes incu-

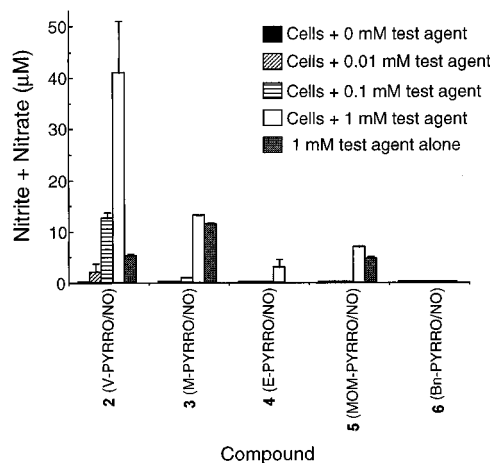


Figure 1. Accumulation of nitric oxide oxidation products during 6 h of incubating *O*²-substituted 1-(pyrrolidin-1-yl)-diazene-1-ium-1,2-diolates **2–6** at 0, 0.01, 0.1, or 1 mM with cultured rat hepatocyte monolayers or at 1 mM in the absence of cells. Data are the means \pm SD of duplicate determinations.

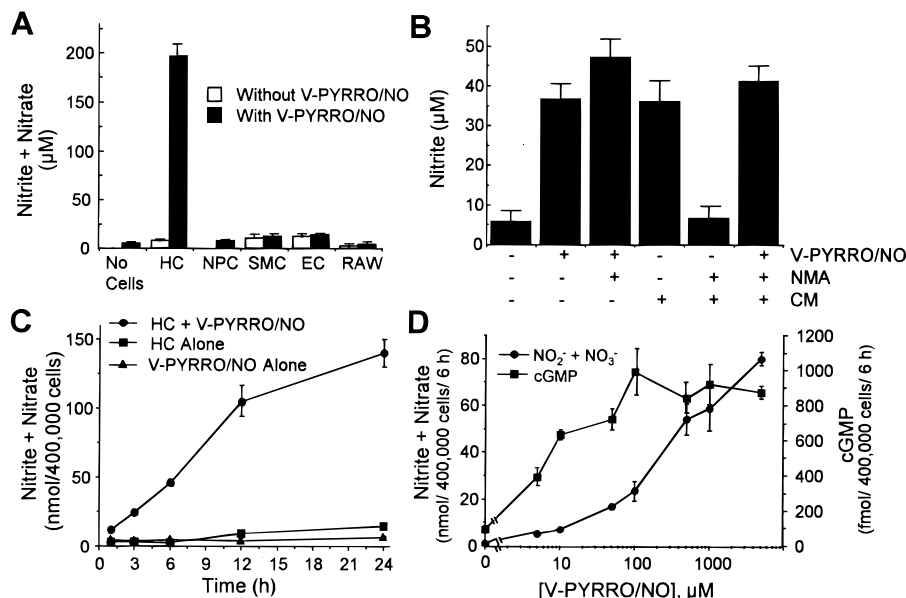


Figure 2. Hepatocyte specificity for NO release from V-PYRRO/NO. (A) The release of nitrite + nitrate from monolayers of cultured rat hepatocytes (HC, 4×10^5 cells/well), rat liver nonparenchymal cells (NPC, 1×10^6 cells/well), rat pulmonary artery smooth muscle cells (SMC, 5×10^5 cells/well), sheep pulmonary artery endothelial cells (EC, 1×10^6 cells/well), and murine RAW 264.7 macrophages (RAW, 1×10^6 cells/well) during 24 h of exposure to 1 mM V-PYRRO/NO is shown. (B) The 24-h release of nitrite alone by HC cultured in the presence of 1 mM V-PYRRO/NO, the NO synthase inhibitor *N*^G-methyl-L-arginine (NMA, 0.5 mM), or a mixture of cytokines (CM: 100 units/mL IL-1 β + 500 units/mL TNF α + 100 units/mL IFN γ), or combinations of these agents. (C) A time course for the release of nitrite + nitrate by cultured HC alone, HC cultured with 1 mM V-PYRRO/NO, and V-PYRRO/NO incubated without cells in culture medium. (D) The 6-h release of nitrite + nitrate and cGMP from HC cultured with increasing concentrations of V-PYRRO/NO.

bated with V-PYRRO/NO was not blocked by the NOS inhibitor *N*^G-methyl-L-arginine (NMA), indicating that activation of an endogenous NOS was not the source of the NO (Figure 2B). Endogenous NO synthesis was easily detected in hepatocytes exposed to the cytokine mixture (CM) consisting of interleukin-1 β (IL-1 β) + tumor necrosis factor- α (TNF α) + interferon- γ (IFN γ), as expected.^{11,12} Stimulation with cytokines did not diminish the metabolism of V-PYRRO/NO to NO, as demonstrated by the release of NO₂⁻ by CM-treated hepatocytes incubated with both NMA and V-PYRRO/NO (Figure 2B). Following the addition of 1 mM V-PYRRO/NO to hepatocytes, NO₂⁻ + NO₃⁻ release remained constant at 8–10 nmol/h/(4×10^5) hepatocytes for the first 12 h and then decreased to 3–5 nmol/h/(4×10^5) hepatocytes for the remaining 12 h (Figure 2C). Concentrations of V-PYRRO/NO as low as 5 μ M stimulated measurable release of cGMP, the product of soluble guanylyl cyclase activation by NO, from hepatocyte cultures. cGMP release became maximal at 100 μ M V-PYRRO/NO, and NO₂⁻ + NO₃⁻ release was maximal at 1 mM (Figure 2D), suggesting that soluble guanylyl cyclase was maximally stimulated by the concentration of NO generated by 100 μ M V-PYRRO/NO. Thus V-PYRRO/NO released NO only in the presence of hepatocytes and then in a sustained manner for 12–24 h, with micromolar concentrations being required for biological activity based on cGMP release *in vitro*.

Selective Metabolism of V-PYRRO/NO to NO in the Liver *in Vivo*

To establish whether V-PYRRO/NO targeted the liver *in vivo*, arterial and venous cannulas were placed in rats anesthetized with pentobarbital, and equimolar boluses

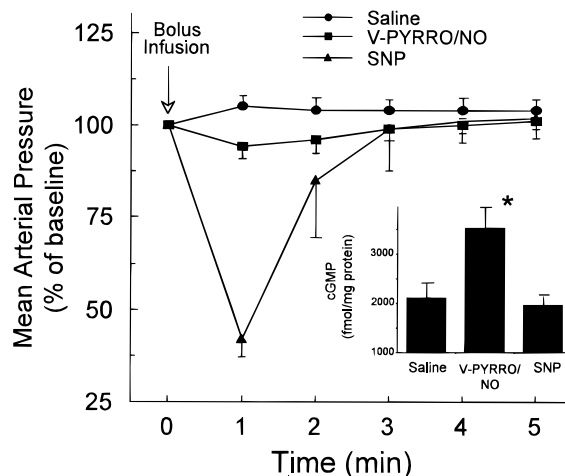


Figure 3. The effects of infusing 0.3 mL of saline alone or saline containing 30 nmol/kg V-PYRRO/NO or sodium nitroprusside (SNP) on mean arterial blood pressure in rats are shown ($N = 5$ per group). The inset shows cGMP levels determined by radioimmunoassay in homogenates of snap-frozen liver tissue obtained from the same animals 5–10 min after the infusion ($*P < 0.05$ vs saline).

of V-PYRRO/NO or the clinical NO-releasing, antihypertensive agent sodium nitroprusside (SNP) were infused intravenously with constant blood pressure monitoring. V-PYRRO/NO caused only a slight drop in mean arterial blood pressure, while SNP caused an immediate, profound decrease in blood pressure (Figure 3). Liver cGMP levels at 5–10 min after the infusion were elevated only in the V-PYRRO/NO group (Figure 3, inset). This experiment indicated that V-PYRRO/NO released biologically active NO in the liver, elevating cGMP levels with minimal effects on systemic blood pressure.

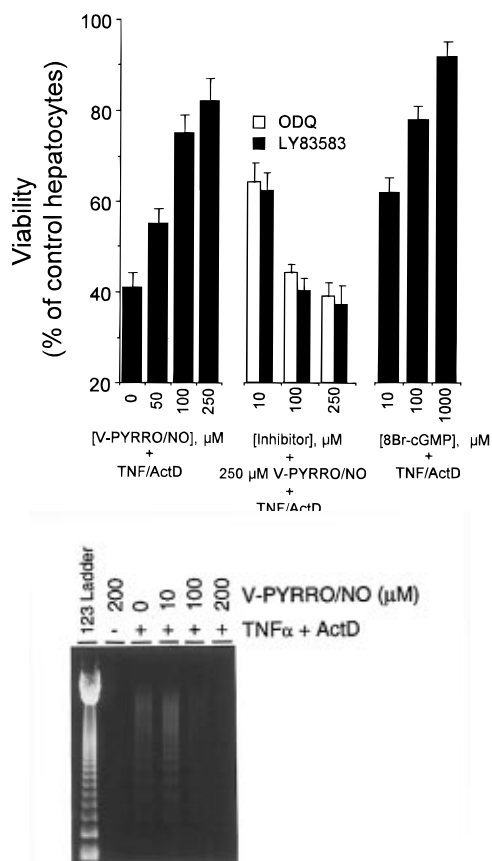


Figure 4. (A, Top) Viability of cultured rat hepatocytes at 12 h after exposure to 40 pg/mL TNF α + 0.5 μ g/mL ActD (TNF/ActD) as determined by crystal violet staining. TNF/ActD-treated hepatocytes were also cultured in the presence of V-PYRRO/NO alone or with the soluble guanylyl cyclase inhibitors 1*H*-[1,2,4]oxadiazolo[4,3-*a*]quinoxalin-1-one (ODQ) or 6-anilino-5,8-quinolinedione (LY83583), or the membrane permeable cGMP analogue 8-bromo-cGMP (8Br-cGMP) in the concentrations shown. (B, Bottom) Apoptosis detected as the presence of fragmented DNA is shown for hepatocytes cultured with TNF/ActD with or without V-PYRRO/NO.

V-PYRRO/NO Protects Hepatocytes from TNF α -Induced Toxicity *in Vitro* and *in Vivo*

The extensive hepatocellular injury of fulminant hepatic failure is thought to be mediated, in part, by cytokines including TNF α .^{13,14} TNF α induces hepatocyte apoptosis, and this toxicity is markedly enhanced in the presence of transcriptional inhibitors such as actinomycin D (ActD) or galactosamine (GalN).¹⁵ V-PYRRO/NO concentrations of 100 μ M or greater dramatically decreased the toxicity of TNF α + ActD (TNF/ActD) in cultured hepatocytes as measured by the crystal violet method (Figure 4A) and confirmed by lactate dehydrogenase release (data not shown). This is the same V-PYRRO/NO concentration which stimulated maximal cGMP release. The protective action of V-PYRRO/NO was mimicked by the cell membrane permeant analogues of cGMP, 8-bromo-cGMP (8Br-cGMP, shown) and dibutyryl cGMP (not shown), at concentrations as low as 10 μ M and blocked by the inhibitors of soluble guanylyl cyclase, 1*H*-[1,2,4]oxadiazolo[4,3-*a*]quinoxalin-1-one (ODQ) and 6-anilino-5,8-quinolinedione (LY83583) (Figure 4A). The protection from toxicity correlated with a reduction in apoptosis as measured by DNA fragmentation (Figure 4B). Compound **6**, a diazeniumdiolate having a benzyl group

instead of a vinyl group bound to the *O*²-position that was not metabolized by hepatocytes (Figure 1), did not protect hepatocytes from TNF/ActD-induced cell death (data not shown). We conclude from these experiments that NO release from V-PYRRO/NO protected hepatocytes from TNF/ActD-induced apoptosis via a mechanism involving cGMP.

To determine if V-PYRRO/NO would block TNF α -mediated liver damage *in vivo*, catheters connected to Alzet osmotic pumps were inserted into the jugular veins of rats to give a constant infusion of V-PYRRO/NO at 1.06 μ mol/kg/h. Apoptotic liver failure was induced by the intraperitoneal injection of 10 μ g/kg TNF α and 700 mg/kg GalN (TNF/GalN). Liver damage was determined at 8 h by the presence of DNA fragmentation as a marker of apoptosis and at 24 h by plasma aspartate aminotransferase (AST) and alanine aminotransferase (ALT) levels. One out of six TNF/GalN-treated animals with saline infusion died while all animals receiving V-PYRRO/NO infusion survived the 24 h. Furthermore, TNF/GalN-treated animals with pumps containing vehicle (saline) all exhibited massive liver damage and apoptosis, while animals receiving a constant infusion of V-PYRRO/NO exhibited essentially no DNA fragmentation and had minimal elevations in plasma AST and ALT levels (Figure 5). The significant reduction in hepatocellular apoptosis in animals with V-PYRRO/NO infusion was confirmed using the TUNEL assay and Hoechst staining on intact liver tissue (not shown).

Discussion

With the aim of developing a method for delivering NO specifically to the liver without affecting other NO-sensitive tissues, we have identified a diazeniumdiolate ion that dissociates to NO particularly rapidly in aqueous media (3 s in pH 7.4 buffer at 37 $^{\circ}$ C) and stabilized it by covalent attachment of protecting groups that the desired target organ's drug-metabolizing enzymes might rapidly remove. This strategy has yielded a promising prodrug, V-PYRRO/NO (**2**), that is indeed liver-selective, increasing cGMP levels in that organ after intravenous administration with little effect on systemic blood pressure.

As one of many research and clinical applications that might be conceived for such an agent, we have shown it to reduce considerably the otherwise extensive hepatocellular death and apoptosis induced on exposure to toxic levels of tumor necrosis factor- α , an effect similar to that seen in some types of fulminant hepatic failure. Relatively high concentrations of V-PYRRO/NO (micromolar range) were required for *in vitro* protection, whereas low quantities of the donor were effective *in vivo*. We speculate that this may be due to slow *in vitro* metabolism of V-PYRRO/NO by the hepatocytes. On the basis of our experimental results, we anticipate that a constant infusion of a low quantity of such a liver-specific NO donor would be both required and adequate to block hepatocellular apoptosis in the clinical setting. Current efforts are focused on determining if local NO delivery can ameliorate liver damage following exposure to hepatotoxicants where liver failure is more gradual in onset.

Several recent studies have shown that NO reduces toxicity associated with apoptosis in other *in vitro*

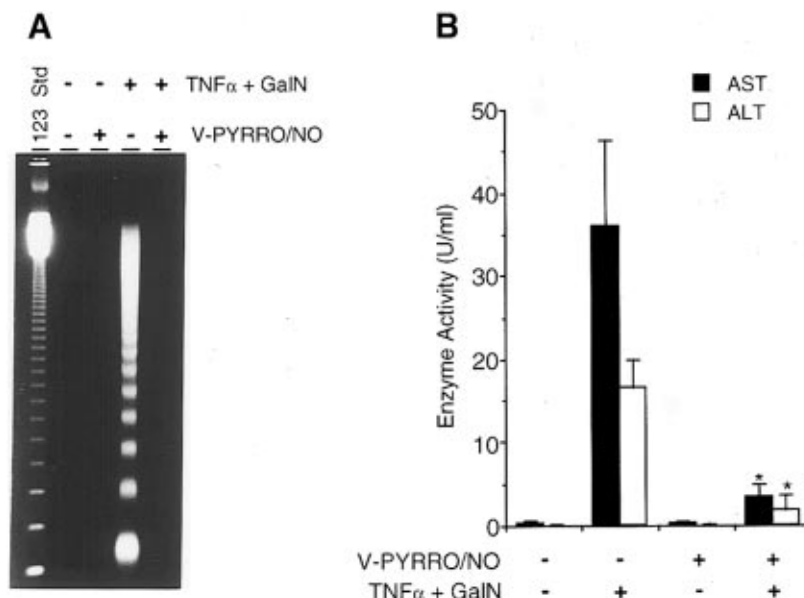


Figure 5. (A) Hepatic apoptosis was determined 8 h after administration of 10 μ g/kg TNF α + 700 mg/kg galactosamine (GalN) to rats with or without constant infusion of V-PYRRO/NO (1.06 μ mol/kg/h) by measuring the presence of fragmented cytosolic DNA in whole liver (data representative of six animals per group). (B) At 24 h, plasma aspartate aminotransferase (AST) and alanine aminotransferase (ALT) levels were determined ($N = 5-6$ per group; * $P < 0.01$ vs TNF α + GalN with saline infusion).

systems. Both cGMP-independent¹⁶ and -dependent¹⁷⁻²⁰ mechanisms of protection have been implicated. Our *in vitro* data show that one mechanism by which NO may protect hepatocytes from TNF α -induced injury is through the stimulation of soluble guanylyl cyclase. It is likely that other mechanisms are also involved. For example, we have shown that NO can protect hepatocytes from apoptosis through heat shock protein induction²¹ and through protein *S*-nitrosylation (unpublished observations), both independent of cGMP. Since TNF α toxicity is thought to include the generation of oxygen radicals,²² it is possible that the antioxidant action of NO may also be involved. Although determination of the protective mechanism will require further experimentation, these studies hold promise for the development of therapeutic approaches using site-specific NO donors to reduce tissue injury.

Significance

Although nitric oxide (NO) can be cytotoxic to some cells,²³⁻²⁹ it is paradoxically cytoprotective for many cell types *in vitro*, including hepatocytes.³⁰⁻³⁴ A mode of protection by NO identified *in vitro* in B-lymphocytes,^{16,17} eosinophils,¹⁸ ovarian follicles,¹⁹ and thymocytes²⁰ is the inhibition of apoptosis. Both cGMP-dependent¹⁷⁻¹⁹ and cGMP-independent¹⁶ antiapoptotic mechanisms have been identified. Apoptotic cell death is thought to contribute to dysfunction or failure *in vivo* in organs such as the heart³⁵ and liver.^{13,15} It has not been feasible previously to exploit the cytoprotective properties of NO to prevent cell death in such conditions, due to unwanted side effects of systemically administered NO-releasing drugs such as hypotension and the toxicity of both NO and its reaction products to susceptible cells. Our synthesis of a molecule capable of delivering therapeutic quantities of NO to the liver without apparent effect on other NO-sensitive parts of the anatomy may provide a means of attenuating the massive hepatocellular damage characteristic of fulminant hepatic failure without systemic effects and obviate

the need for more radical therapies such as liver transplantation. This and other potential applications of the organ-selective NO delivery strategy introduced here are under active investigation.

Experimental Section

Warning! Many of the reagents used in this work, including methyl chloromethyl ether and the other alkylating agents, are potentially toxic and should be handled, stored, and discarded with due respect for the potential hazards involved.

Proton NMR spectra were recorded using a Varian XL-200 with advance data system. Spectra were obtained in deuteriochloroform unless otherwise indicated. Chemical shifts (δ) are reported in parts per million downfield from tetramethylsilane. Mass spectral measurements were carried out in the electron impact mode (except as otherwise noted) on a VG-Micromass Model 7070 spectrometer. Ultraviolet (UV) spectra were run as aqueous solutions (except as otherwise noted) on a Hewlett-Packard 8451A diode array spectrophotometer. Progress of most reactions was monitored on a Varian Model 3700 gas chromatograph using a 30-m \times 0.25-mm HeliFlex Bonded/FSOT/Superx capillary column (Alltech Associates, Deerfield, IL). Flash chromatography was performed on a Flash 40 System (Biotage, Inc., Charlottesville, VA) using a 4.0 \times 15-cm KP-Sil (silica gel) column with elution at 15 psi of air and a flow rate of 25 mL/min. Elemental analysis data were provided by Atlantic Microlab, Inc. (Norcross, GA) or SRI International (Palo Alto, CA). *N*-Methyl-L-arginine (NMA) was purchased from Chem-Biochem Research, Inc. (Salt Lake City, UT). Interleukin-1 β (IL-1 β) was supplied by the National Cancer Institute's Biological Resources Branch (Frederick, MD). Interferon- γ (IFN γ) was obtained from Gibco (Grand Island, NY). Recombinant murine tumor necrosis factor- α (TNF α) was purchased from Genzyme (Cambridge, MA). Actinomycin D (ActD), 3-isobutyl-1-methylxanthine (IBMX), cyclic 8-bromoguanosine 3',5'-cyclic monophosphate (8Br-cGMP), and D-galactosamine (GalN) were provided by Sigma Chemical Co. (St. Louis, MO). 1*H*-[1,2,4]Oxadiazolo[4,3-*a*]quinoxalin-1-one (ODQ) was from Tocris Cookson, St. Louis, MO. 6-Anilino-5,8-quinolinedione (LY83583) was purchased from Alexis Corp., San Diego, CA.

Pyrrolidinium 1-(Pyrrolidin-1-yl)diazene-1-ium-1,2-diolate. A solution of 36 g (0.51 mol) of pyrrolidine in 50 mL of ether and 25 mL of acetonitrile was placed in a 500-mL Parr bottle, degassed, and charged with 3 atm of nitric oxide. The

reactor was cooled to $-80\text{ }^{\circ}\text{C}$. After 4 h the pressure was released and the crystalline product was collected by filtration with a fritted glass funnel and then washed with cold ether under an atmosphere of nitrogen. The material was dried in a vacuum desiccator at 1 mmHg and $25\text{ }^{\circ}\text{C}$ for 3 h to give 23 g (45%) of white needles: mp $73\text{--}74\text{ }^{\circ}\text{C}$. Anal. ($\text{C}_8\text{H}_{18}\text{N}_4\text{O}_2$) C, H, N.

The pyrrolidinium salt decomposed very rapidly on dissolution in methanol- d_4 , so no useful NMR data were obtained. Accordingly, it was converted to the more stable sodium salt for subsequent work by treatment with 10 M sodium hydroxide. After flooding the resulting mixture with ether (250 mL), the solid sodium salt was collected by filtration.

Alternatively, the sodium salt could be prepared directly as follows.

Sodium 1-(Pyrrolidin-1-yl)diazen-1-ium-1,2-diolate (1). A solution of 28.2 g (0.397 mol) of pyrrolidine in 100 mL of acetonitrile and 100 mL of ether was mixed with 94 mL (0.4 mol) of 25% sodium methoxide in methanol. The resulting solution was flushed with nitrogen, charged with 40 psi of NO, and stirred at room temperature. A thick precipitate began to form within 1 h of exposure to NO. Two days later, the pressure was released and the product was collected by filtration, washed with ether, and dried under vacuum to give 32.1 g (54%) of a white powder: NMR (D_2O) δ 1.91 (m, 4 H), 3.22 (m, 4 H); UV (0.01 M NaOH) λ_{max} (ϵ) 252 nm ($8.8\text{ mM}^{-1}\text{ cm}^{-1}$); half-lives 8.5 s at $25\text{ }^{\circ}\text{C}$ and 2.8 s at $37\text{ }^{\circ}\text{C}$ in pH 7.4 phosphate buffer. Anal. ($\text{C}_4\text{H}_8\text{N}_3\text{O}_2\text{Na}$) H, N; C: calcd, 31.38; found, 33.50; Na: calcd, 15.00; found, 17.37.

***O*-Vinyl 1-(Pyrrolidin-1-yl)diazen-1-ium-1,2-diolate (2).** To a solution of 1.2 g (5 mmol) of *O*-(2-bromoethyl) 1-(pyrrolidin-1-yl)diazen-1-ium-1,2-diolate (**7**, preparation described below) in 50 mL of tetrahydrofuran was added 5 g of powdered sodium hydroxide and 0.5 mL of water. The reaction mixture was heated at reflux overnight, allowed to cool to room temperature, and concentrated on a rotary evaporator. The residue was extracted with dichloromethane, dried over sodium sulfate, filtered, and evaporated. Purification was carried out on a silica gel column (or, more efficiently, by flash chromatography) with dichloromethane as eluant to give 423 mg of product as a pale yellow oil: NMR δ 1.98 (m, 4 H), 3.62 (m, 4 H), 4.34 (dd, 1 H), 4.81 (dd, 1 H), 6.78 (dd, 1 H); UV λ_{max} (ϵ) 268 nm ($9.7\text{ mM}^{-1}\text{ cm}^{-1}$); MS m/z (relative intensity) 157 (M^+ , 7), 130 (27), 101 (100), 100 (58), 85 (14), 84 (45), 70 (16), 56 (23). Anal. ($\text{C}_6\text{H}_{11}\text{N}_3\text{O}_2$) C, H, N.

***O*-Methyl 1-(Pyrrolidin-1-yl)diazen-1-ium-1,2-diolate (3).** A slurry of 2.6 g (0.017 mol) of **1** and 2 g of anhydrous sodium carbonate in 50 mL of methanol was cooled to $0\text{ }^{\circ}\text{C}$ under a nitrogen atmosphere. To the stirred mixture was added 2.4 mL (0.025 mol) of dimethyl sulfate (dropwise). The solution was kept cold for 1 h and then warmed to room temperature for an additional hour. To the reaction mixture was added 10 mL of 10% aqueous sodium hydroxide, and the solution was stirred for 30 min to decompose any unreacted dimethyl sulfate. Most of the solvent was removed on a rotary evaporator, and the residue was extracted with dichloromethane. The solution was dried over sodium sulfate and filtered through magnesium sulfate. The solvent was evaporated to give 1.25 g of a yellow oil. Purification of the crude material was carried out on silica gel (200–400 mesh) eluted with dichloromethane then 5:1 dichloromethane:ethyl acetate to give 819 mg (33%) of *O*-methyl 1-(pyrrolidin-1-yl)diazen-1-ium-1,2-diolate: bp $76\text{--}77\text{ }^{\circ}\text{C}$ at 0.5 mmHg; NMR δ 1.95 (m, 4 H), 3.54 (m, 4 H), 3.97 (s, 3 H); UV λ_{max} (ϵ) 254 nm ($7.9\text{ mM}^{-1}\text{ cm}^{-1}$); MS m/z (relative intensity) 145 (M^+ , 8), 130 (32), 100 (100), 70 (18), 69 (7), 68 (12), 56 (10), 55 (6). Anal. ($\text{C}_5\text{H}_{11}\text{N}_3\text{O}_2$) C, H, N.

***O*-Ethyl 1-(Pyrrolidin-1-yl)diazen-1-ium-1,2-diolate (4).** This preparation was carried out as described above for the methyl analog. Diethyl sulfate was used here as the alkylating agent to give a 40% yield of pure *O*-ethyl 1-(pyrrolidin-1-yl)diazen-1-ium-1,2-diolate: bp $58\text{ }^{\circ}\text{C}$ at 0.2 mmHg; NMR δ 1.37 (t, 3 H), 1.94 (m, 4 H), 4.24 (q, 2 H), 5.53 (m, 4 H); UV λ_{max} (ϵ) 254 nm ($9.0\text{ mM}^{-1}\text{ cm}^{-1}$); MS m/z (relative intensity) 159 (M^+ , 2), 130 (9), 101 (100), 100 (40), 70 (14), 56 (9), 56 (9), 55 (65). Anal. ($\text{C}_6\text{H}_{13}\text{N}_3\text{O}_2$) C, H, N.

***O*-Methoxymethyl 1-(Pyrrolidin-1-yl)diazen-1-ium-1,2-diolate (5).** A slurry of 4.3 g (0.028 mol) of **1** and 3 g of anhydrous sodium carbonate in 100 mL of tetrahydrofuran was cooled to $0\text{ }^{\circ}\text{C}$ in an ice bath. To this was added 2.7 mL (0.035 mol) of methyl chloromethyl ether followed by the dropwise addition of 10 mL of methanol. The ice bath was removed, and the reaction mixture was stirred at room temperature under nitrogen for 18 h. After filtration, the filtrate was washed with brine, dried over sodium sulfate, filtered through a layer of magnesium sulfate, and evaporated to give 2.85 g of a yellow oil. Purification on silica gel using 5:1 dichloromethane:ethyl acetate as the eluant gave 1.45 g (30%) of *O*-methoxymethyl 1-(pyrrolidin-1-yl)diazen-1-ium-1,2-diolate: bp $105\text{ }^{\circ}\text{C}$ at 0.55 mmHg; NMR δ 1.95 (m, 4 H), 3.50 (s, 3 H), 3.59 (m, 4 H), 5.18 (s, 2 H); UV λ_{max} (ϵ) 256 nm ($7.6\text{ mM}^{-1}\text{ cm}^{-1}$); MS (chemical ionization positive ion spectrum, NH_3) m/z (relative intensity) 193 ($\text{M} + \text{NH}_4^+$, 21), 176 (MH^+ , 50), 145 (57), 115 (57), 115 (20), 101 (100), 84 (21), 70 (29), 56 (4), 45 (48). Anal. ($\text{C}_6\text{H}_{13}\text{N}_3\text{O}_3$) C, H, N.

***O*-Benzyl 1-(Pyrrolidin-1-yl)diazen-1-ium-1,2-diolate (6).** A slurry of 1.93 g (0.0126 mol) of **1** in 50 mL of tetrahydrofuran was cooled to $0\text{ }^{\circ}\text{C}$. To the cold mixture were added 1.43 mL (0.012 mol) of benzyl bromide and 10 mL of *N,N*-dimethylformamide. The reaction mixture was allowed to warm to room temperature and stirred under nitrogen for 48 h. The solution was concentrated on a rotary evaporator, treated with 150 mL of water, and extracted with ether. The organic layer was washed with aqueous sodium bisulfite solution, dried over sodium sulfate, filtered through a layer of magnesium sulfate, and evaporated to give 1.63 g of a yellow oil. The crude material was chromatographed on silica gel and eluted with 5:1 dichloromethane:ethyl acetate to give 1.54 g of product: NMR δ 1.91 (m, 4 H), 3.49 (m, 4 H), 5.17 (s, 2 H), 7.36 (m, 5 H); UV (ethanol) λ_{max} (ϵ) 256 nm ($8.2\text{ mM}^{-1}\text{ cm}^{-1}$); MS (liquid secondary ion mass spectrometry with a VG Micromass ZAB-2F instrument; matrix, glycerol + sodium iodide) m/z (relative intensity) 244 ($\text{M}^+ + 23$, 100), 221 (6), 191 (9), 173 (10), 147 (17), 133 (34), 123 (28). Anal. ($\text{C}_{11}\text{H}_{15}\text{N}_3\text{O}_2$) C, H, N.

***O*-(2-Bromoethyl) 1-(Pyrrolidin-1-yl)diazen-1-ium-1,2-diolate (7).** A slurry of 12.2 g (0.0797 mol) of **1** in 100 mL of tetrahydrofuran was cooled to $0\text{ }^{\circ}\text{C}$ in an ice bath, whereupon 3 g of anhydrous sodium carbonate was added followed by 8.63 mL (0.1 mol) of 1,2-dibromoethane in 20 mL of dimethyl sulfoxide. The reaction mixture was allowed to warm to room temperature and stirred under nitrogen for 72 h. The reaction mixture was cooled in an ice bath and treated with 200 mL of distilled water, extracted with ether, washed with aqueous sodium bisulfite solution, dried, and evaporated. The product was chromatographed on silica gel and eluted with 5:1 dichloromethane:ethyl acetate (or, more efficiently, by flash chromatography on elution with 1:1 cyclohexane:ethyl acetate), yielding 1.54 g of pure product: NMR δ 1.96 (m, 4 H), 3.61 (t, 2 H), 3.66 (m, 4 H), 4.43 (t, 2 H); UV λ_{max} (ϵ) 254 nm ($6.2\text{ mM}^{-1}\text{ cm}^{-1}$); MS m/z (relative intensity) 239 (M^+ , ^{81}Br , 5), 237 (M^+ , ^{79}Br , 6), 209 (19), 207 (20), 130 (32), 109 (38), 107 (35), 101 (64), 100 (100), 70 (40), 55 (25), 43 (35). Anal. ($\text{C}_6\text{H}_{12}\text{N}_3\text{O}_2$ Br) C, H, N, Br.

Cell Isolation and Culture. Liver cells were obtained from male Sprague–Dawley rats. Hepatocytes were isolated using a collagenase digestion method as described.³⁶ The hepatocytes were purified over a 30% Percoll gradient and cultured on collagen-coated 12-well plastic tissue culture dishes at 4×10^5 cells/well for 24 h prior to the addition of test substances. Liver nonparenchymal cells comprised of endothelial cells and Kupffer cells were obtained by using a Pronase E digestion of the parenchyma as described³⁷ and cultured at 1×10^6 cells/well on 12-well plastic tissue culture trays for 24 h prior to treatment. Rat pulmonary artery smooth muscle cells were isolated from artery explants as described.³⁸ The cells stained positive for α -actin and smooth muscle myosin, and were cultured in DMEM/F12 (1:1 v/v) and 10% fetal calf serum. Only passages 3–8 were used and were grown to subconfluence on 12-well plastic tissue culture trays. Sheep pulmonary artery endothelial cells were obtained by collagenase digestion³⁹ and purified after second passage by

fluorescence-activated cell sorting using 1,1'-dioctadecyl-3,3,3',3'-tetramethylindocarbocyanine perchlorate-labeled acetylated low-density lipoprotein (Biomedical Technologies Inc., Oklahoma City, OK) to identify endothelial cells. Subconfluent cultures on 12-well culture trays, passages 3–8, were used for all experiments.

Assays. Nitrite was measured using the Griess reaction. Where nitrate was also measured, the nitrate was first converted to nitrite using copper-coated cadmium as described.⁴⁰ Viability of cultured hepatocytes was determined using crystal violet staining as described.⁴¹

In Vivo Experiments. *Technical alert!* We believe it is important to keep the concentration of V-PYRRO/NO in aqueous injection solutions at or below its solubility limit of 5 mg/mL. If this limit is exceeded, highly concentrated microparticles can form, leading to uneven dose rates, local inhomogeneities in distribution pattern, and potentially lethal toxic effects. In experiments with osmotic pumps, we have also noted that aqueous mixtures containing more than 5 mg/mL of V-PYRRO/NO can weaken and rupture the pump wall (presumably reflecting either blockage of the orifice by the microparticles or strong penetrating and solubilizing properties on the part of V-PYRRO/NO) after implantation. We have experienced no problems at V-PYRRO/NO concentrations of 5 mg/mL or less, however.

Male Sprague–Dawley rats each weighing 250–300 g (Harlan Sprague–Dawley, Indianapolis, IN) were used in all *in vivo* experiments in accordance with the guidelines of the University of Pittsburgh Animal Care and Use Committee. To measure the effect of V-PYRRO/NO on the mean arterial blood pressure (MAP), rats were anesthetized with intraperitoneal pentobarbital (30 mg/kg), the tracheas were cannulated, and the animals were ventilated using a rodent ventilator. The right jugular vein and the left common carotid artery were cannulated with heparinized PE-50 tubing for test agent infusion and continuous MAP monitoring, respectively. Once the blood pressure had stabilized, 0.3 mL of saline alone, or ~0.3 mL of saline containing enough V-PYRRO/NO or sodium nitroprusside to provide a dose of 30 nmol/kg, was infused and the MAP was recorded every 30 s for 5 min using a blood pressure analyzer (Micro-Med, Inc., Louisville, KY). The abdomen was then opened, the aorta was cannulated, and the line was flushed with ice-cold saline containing the phosphodiesterase inhibitor 3-isobutyl-1-methylxanthine (IBMX) (0.25 mM). A section of liver was removed, snap-frozen, and stored at –80 °C until it could be analyzed for cGMP content.

To test the capacity of V-PYRRO/NO to inhibit apoptosis in the liver *in vivo*, rats were anesthetized with pentobarbital and Alzet osmotic minipumps (Model 2001 D, Alzet Co., Palo Alto, CA) were implanted subcutaneously on the dorsum of the animal. PE-10 tubing flushed with the same solution used in the pump was inserted into the jugular vein and connected to the pump via a subcutaneous tunnel. All pumps were placed in a water bath at 37 °C prior to insertion to assure immediate infusion when placed in the animal. Following pump placement, rats were injected intraperitoneally with 10 µg/kg of TNF α and 700 mg/kg of GalN. Eight or 24 h later, animals were placed under inhaled isoflurane anesthesia for isolation of plasma and liver tissue. The latter was snap-frozen and stored at –80 °C until it was assessed for the presence of apoptosis. Plasma was stored at –80 °C until it was analyzed for AST and ALT levels. Plasma levels of alanine aminotransferase (ALT) and aspartate aminotransferase (AST), and supernatant levels of lactate dehydrogenase (LDH), were measured by an automated method using a Technitron RA 500 analyzer. cGMP levels were determined by radioimmunoassay using a commercially available kit (Amersham, Cambridge, MA).

DNA Fragment Assay. Enriched low molecular weight DNA from whole liver tissue was isolated and extracted according to modifications of the methods of Wyllie⁴² as well as Hughes and Gorospe.⁴³ Whole frozen liver tissue was homogenized in ice-cold lysis buffer (5 mM Tris, 20 mM EDTA, 0.5% Triton X-100, pH 8.0). Following the addition of diethyl pyrocarbonate (DEPC, Sigma Chemical Co., St. Louis, MO; final concentration = 0.2% v/v) to inhibit endogenous nuclease

activity, homogenates were incubated on ice for 90 min with occasional mixing. The homogenate was then centrifuged at 27000g for 20 min to separate fragmented DNA and subjected to proteinase K digestion (0.5 mg/mL, 1 h at 37 °C) followed by repeated phenol:chloroform extraction. Nucleic acids were precipitated with 100% ethanol at –20 °C, collected by centrifugation at 15000g, and subjected to ribonuclease A (2.5 µg/mL) treatment. Samples were extracted, precipitated as above, and dried. Nucleic acid pellets were resuspended in TE buffer (10 mM Tris, 1 mM EDTA, pH 8.0). The concentration and purity of DNA were estimated spectrophotometrically by the ratio of absorbances at 260 and 280 nm. Samples (~50 µg of DNA) were mixed with gel loading buffer (0.05% w/v bromophenol blue, 40% w/v sucrose, 0.1 M EDTA, pH 8.0) and electrophoresed on 2% agarose gels at 50 V in TAE buffer (40 mM Tris, 5 mM sodium acetate, 1 mM EDTA, pH 7.6). Gels were stained with ethidium bromide and visualized by ultraviolet transillumination. A double-stranded 123-bp DNA ladder served as a standard.

Light Microscopic Detection of Apoptosis. To analyze both the number and morphology of the apparently apoptotic cells within the cell population, we used light fluorescent microscopy methods. Cryosections of fixed, frozen livers were cut, mounted on slides, and labeled using the TUNEL assay. This assay specifically detects ladder DNA by terminal tailing of DNA with fluorescently tagged bases. DNA strand breaks were directly labeled by incubating sections with 0.15 nM fluorescein-12-dUTP (Boehringer Mannheim, Indianapolis, IN) and terminal deoxynucleotidyl transferase (200 units/mL, Stratagene, La Jolla, CA) in reaction buffer. Cobalt was added to enhance labeling of protruding, recessed, and blunt DNA breaks containing a free 3'-OH. After 45 min at 37 °C, the reaction was terminated by washing with phosphate-buffered saline, and the specimen was counterstained with a 2 mg/mL solution of Hoechst 33258 (Sigma) for 3 min. This stain specifically stains DNA and allows all nuclei in the section, or the entire section, to be examined. The cells were then mounted in Gelvatol (Monsanto, St. Louis, MO) and observed using a Nikon FXL photomicroscope. Random images using a 60 \times objective were collected using a 3 Chip Sony color camera. The apoptotic nuclei in each field were counted, and the types of apoptotic cells were classified.

Acknowledgment. We thank Keith Davies and Dorris Taylor for determining the decomposition rates of **1**. Research was supported in part by NIH Grants R01-GM-44100 and R01-GM-37753. T.R.B. is the recipient of the George H. A. Clowes Jr., MD FACS Memorial Research Career Development Award of the American College of Surgeons.

References

- (1) Kerwin, J. F., Jr.; Lancaster, J. R., Jr.; Feldman, P. L. Nitric Oxide: A New Paradigm for Second Messengers. *J. Med. Chem.* **1995**, *38*, 4343–4362.
- (2) Hanson, S. R.; Hutsell, T. C.; Keefer, L. K.; Mooradian, D. L.; Smith, D. J. Nitric Oxide Donors: A Continuing Opportunity in Drug Design. *Adv. Pharmacol.* **1995**, *34*, 383–398.
- (3) Smith, D. J.; Chakravarthy, D.; Pulfer, S.; Simmons, M. L.; Hrabie, J. A.; Citro, M. L.; Saavedra, J. E.; Davies, K. M.; Hutsell, T. C.; Mooradian, D. L.; Hanson, S. R.; Keefer, L. K. Nitric Oxide-Releasing Polymers Containing the [N(O)NO]⁻ Group. *J. Med. Chem.* **1996**, *39*, 1148–1156.
- (4) Saavedra, J. E.; Southan, G. J.; Davies, K. M.; Lundell, A.; Markou, C.; Hanson, S. R.; Adrie, C.; Hurford, W. E.; Zapol, W. M.; Keefer, L. K. Localizing Antithrombotic and Vasodilatory Activity with a Novel, Ultrafast Nitric Oxide Donor. *J. Med. Chem.* **1996**, *39*, 4361–4365.
- (5) Keefer, L. K.; Nims, R. W.; Davies, K. M.; Wink, D. A. "NON-Oates" (1-Substituted Diazen-1-ium-1,2-diolates) as Nitric Oxide Donors: Convenient Nitric Oxide Dosage Forms. *Methods Enzymol.* **1996**, *268*, 281–293.
- (6) Saavedra, J. E.; Dunams, T. M.; Flippen-Anderson, J. L.; Keefer, L. K. Secondary Amine/Nitric Oxide Complex Ions, R₂N[N(O)NO]⁻. O-Functionalization Chemistry. *J. Org. Chem.* **1992**, *57*, 6134–6138.
- (7) Guengerich, F. P. Metabolic Reactions: Types of Reactions of Cytochrome P450 Enzymes. *Handb. Exp. Pharmacol.* **1993**, *105*, 89–103.

- (8) Massey, T. E.; Stewart, R. K.; Daniels, J. M.; Liu, L. Biochemical and Molecular Aspects of Mammalian Susceptibility to Aflatoxin B₁ Carcinogenicity. *Proc. Soc. Exp. Biol. Med.* **1995**, *208*, 213–227.
- (9) Ota, K.; Hammock, B. D. Cytosolic and Microsomal Epoxide Hydrolases: Differential Properties in Mammalian Liver. *Science* **1980**, *207*, 1479–1481.
- (10) Stadler, J.; Bergonia, H. A.; Di Silvio, M.; Sweetland, M. A.; Billiar, T. R.; Simmons, R. L.; Lancaster, J. R., Jr. Nonheme Iron-Nitrosyl Complex Formation in Rat Hepatocytes: Detection by Electron Paramagnetic Resonance Spectroscopy. *Arch. Biochem. Biophys.* **1993**, *302*, 4–11.
- (11) Geller, D. A.; Nussler, A. K.; Di Silvio, M.; Lowenstein, C. J.; Shapiro, R. A.; Wang, S. C.; Simmons, R. L.; Billiar, T. R. Cytokines, Endotoxin, and Glucocorticoids Regulate the Expression of Inducible Nitric Oxide Synthase in Hepatocytes. *Proc. Natl. Acad. Sci. U.S.A.* **1993**, *90*, 522–526.
- (12) Geller, D. A.; de Vera, M. E.; Russell, D. A.; Shapiro, R. A.; Nussler, A. K.; Simmons, R. L.; Billiar, T. R. A Central Role for IL-1 β in the In Vitro and In Vivo Regulation of Hepatic Inducible Nitric Oxide Synthase. IL-1 β Induces Hepatic Nitric Oxide Synthase. *J. Immunol.* **1995**, *155*, 4890–4898.
- (13) Gantner, F.; Leist, M.; Jilg, S.; Germann, P. G.; Freudenberg, M. A.; Tiegs, G. Tumor Necrosis Factor-Induced Hepatic DNA Fragmentation as an Early Marker of T Cell-Dependent Liver Injury in Mice. *Gastroenterology* **1995**, *109*, 166–176.
- (14) Wang, J. H.; Redmond, H. P.; Watson, R. W. G.; Bouchier-Hayes, D. Role of Lipopolysaccharide and Tumor Necrosis Factor- α in Induction of Hepatocyte Necrosis. *Am. J. Physiol.* **1995**, *269*, G297–G304.
- (15) Leist, M.; Gantner, F.; Bohlinger, I.; Germann, P. G.; Tiegs, G.; Wendel, A. Murine Hepatocyte Apoptosis Induced In Vitro and In Vivo by TNF- α Requires Transcriptional Arrest. *J. Immunol.* **1994**, *153*, 1778–1788.
- (16) Mannick, J. B.; Asano, K.; Izumi, K.; Kieff, E.; Stamler, J. S. Nitric Oxide Produced by Human B Lymphocytes Inhibits Apoptosis and Epstein-Barr Virus Reactivation. *Cell* **1994**, *79*, 1137–1146.
- (17) Genaro, A. M.; Hortelano, S.; Alvarez, A.; Martínez-A., C.; Boscá, L. Splenic B Lymphocyte Programmed Cell Death Is Prevented by Nitric Oxide Release Through Mechanisms Involving Sustained Bcl-2 Levels. *J. Clin. Invest.* **1995**, *95*, 1884–1890.
- (18) Beauvais, F.; Michel, L.; Dubertret, L. The Nitric Oxide Donors, Azide and Hydroxylamine, Inhibit the Programmed Cell Death of Cytokine-Deprived Human Eosinophils. *FEBS Lett.* **1995**, *361*, 229–232.
- (19) Chun, S.-Y.; Eisenhauer, K. M.; Minami, S.; Billig, H.; Perlas, E.; Hsueh, A. J. W. Hormonal Regulation of Apoptosis in Early Antral Follicles: Follicle-Stimulating Hormone as a Major Survival Factor. *Endocrinology* **1996**, *137*, 1447–1456.
- (20) Matthys, P.; Froyen, G.; Verdot, L.; Huang, S.; Sobis, H.; Van Damme, J.; Vray, B.; Aguet, M.; Billiau, A. IFN- γ Receptor-Deficient Mice are Hypersensitive to the Anti-CD3-Induced Cytokine Release Syndrome and Thymocyte Apoptosis. Protective Role of Endogenous Nitric Oxide. *J. Immunol.* **1995**, *155*, 3823–3829.
- (21) Kim, Y.-M.; de Vera, M. E.; Watkins, S. C.; Billiar, T. R. Nitric Oxide Protects Cultured Rat Hepatocytes from Tumor Necrosis Factor- α -Induced Apoptosis by Inducing Heat Shock Protein 70 Expression. *J. Biol. Chem.* **1997**, *272*, 1402–1411.
- (22) Goossens, V.; Grooten, J.; De Vos, K.; Fiers, W. Direct Evidence for Tumor Necrosis Factor-Induced Mitochondrial Reactive Oxygen Intermediates and Their Involvement in Cytotoxicity. *Proc. Natl. Acad. Sci. U.S.A.* **1995**, *92*, 8115–8119.
- (23) Albina, J. E.; Cui, S.; Mateo, R. B.; Reichner, J. S. Nitric Oxide-Mediated Apoptosis in Murine Peritoneal Macrophages. *J. Immunol.* **1993**, *150*, 5080–5085.
- (24) Xie, K.; Dong, Z.; Fidler, I. J. Activation of Nitric Oxide Synthase Gene for Inhibition of Cancer Metastasis. *J. Leukocyte Biol.* **1996**, *59*, 797–803.
- (25) Nishio, E.; Fukushima, K.; Shiozaki, M.; Watanabe, Y. Nitric Oxide Donor SNAP Induces Apoptosis in Smooth Muscle Cells Through cGMP-Independent Mechanism. *Biochem. Biophys. Res. Commun.* **1996**, *221*, 163–168.
- (26) Fukuo, K.; Hata, S.; Suhara, T.; Nakahashi, T.; Shinto, Y.; Tsujimoto, Y.; Morimoto, S.; Ogihara, T. Nitric Oxide Induces Upregulation of Fas and Apoptosis in Vascular Smooth Muscle. *Hypertension* **1996**, *27*, 823–826.
- (27) Brüne, B.; Messmer, U. K.; Sandau, K. The Role of Nitric Oxide in Cell Injury. *Toxicol. Lett.* **1995**, *82/83*, 233–237.
- (28) Le, W.-D.; Colom, L. V.; Xie, W.-j.; Smith, R. G.; Alexianu, M.; Appel, S. H. Cell Death Induced by β -Amyloid 1–40 in MES 23.5 Hybrid Clone: The Role of Nitric Oxide and NMDA-Gated Channel Activation Leading to Apoptosis. *Brain Res.* **1995**, *686*, 49–60.
- (29) Xie, K.; Huang, S.; Dong, Z.; Gutman, M.; Fidler, I. J. Direct Correlation Between Expression of Endogenous Inducible Nitric Oxide Synthase and Regression of M5076 Reticulum Cell Sarcoma Hepatic Metastases in Mice Treated with Liposomes Containing Lipopeptide CGP 31362. *Cancer Res.* **1995**, *55*, 3123–3131.
- (30) Wink, D. A.; Hanbauer, I.; Krishna, M. C.; DeGraff, W.; Gamson, J.; Mitchell, J. B. Nitric Oxide Protects Against Cellular Damage and Cytotoxicity from Reactive Oxygen Species. *Proc. Natl. Acad. Sci. U.S.A.* **1993**, *90*, 9813–9817.
- (31) Farinelli, S. E.; Park, D. S.; Greene, L. A. Nitric Oxide Delays the Death of Trophic Factor-Deprived PC12 Cells and Sympathetic Neurons by a cGMP-Mediated Mechanism. *J. Neurosci.* **1996**, *16*, 2325–2334.
- (32) Kim, Y.-M.; Bergonia, H.; Lancaster, J. R., Jr. Nitrogen Oxide-Induced Autoprotection in Isolated Rat Hepatocytes. *FEBS Lett.* **1995**, *374*, 228–232.
- (33) Bohlinger, I.; Leist, M.; Barsig, J.; Uhlig, S.; Tiegs, G.; Wendel, A. Interleukin-1 and Nitric Oxide Protect Against Tumor Necrosis Factor α -Induced Liver Injury Through Distinct Pathways. *Hepatology* **1995**, *22*, 1829–1837.
- (34) Martín-Sanz, P.; Díaz-Guerra, M. J. M.; Casado, M.; Boscá, L. Bacterial Lipopolysaccharide Antagonizes Transforming Growth Factor β 1-Induced Apoptosis in Primary Cultures of Hepatocytes. *Hepatology* **1996**, *23*, 1200–1207.
- (35) Narula, J.; Haider, N.; Virmani, R.; DiSalvo, T. G.; Kolodgie, F. D.; Hajjar, R. J.; Schmidt, U.; Semigran, M. J.; Dec, G. W.; Khaw, B. A. Apoptosis in Myocytes in End-Stage Heart Failure. *N. Engl. J. Med.* **1996**, *335*, 1182–1189.
- (36) Seglen, P. O. Preparation of Isolated Rat Liver Cells. *Methods Cell Biol.* **1976**, *13*, 29–83.
- (37) Emeis, J. J.; Planqué, B. Heterogeneity of Cells Isolated from Rat Liver by Pronase Digestion: Ultrastructure, Cytochemistry and Cell Culture. *J. Reticuloendothel. Soc.* **1976**, *20*, 11–29.
- (38) Davies, P.; Patton, W. Peripheral and Central Vascular Smooth Muscle Cells from Rat Lung Exhibit Different Cytoskeletal Protein Profiles but Similar Growth Factor Requirements. *J. Cell. Physiol.* **1994**, *159*, 399–406.
- (39) Tzeng, E.; Shears, L. L., II; Robbins, P. D.; Pitt, B. R.; Geller, D. A.; Watkins, S. C.; Simmons, R. L.; Billiar, T. R. Vascular Gene Transfer of the Human Inducible Nitric Oxide Synthase: Characterization of Activity and Effects on Myointimal Hyperplasia. *Mol. Med.* **1996**, *2*, 211–225.
- (40) Stuehr, D. J.; Marletta, M. A. Mammalian Nitrate Biosynthesis: Mouse Macrophages Produce Nitrite and Nitrate in Response to *Escherichia coli* Lipopolysaccharide. *Proc. Natl. Acad. Sci. U.S.A.* **1985**, *82*, 7738–7742.
- (41) Meager, A.; Leung, H.; Woolley, J. Assays for Tumour Necrosis Factor and Related Cytokines. *J. Immunol. Methods* **1989**, *116*, 1–17.
- (42) Wyllie, A. H. Glucocorticoid-Induced Thymocyte Apoptosis Is Associated with Endogenous Endonuclease Activation. *Nature* **1980**, *284*, 555–556.
- (43) Hughes, F. M., Jr.; Gorospe, W. C. Biochemical Identification of Apoptosis (Programmed Cell Death) in Granulosa Cells: Evidence for a Potential Mechanism Underlying Follicular Atresia. *Endocrinology* **1991**, *129*, 2415–2422.

JM9701031